Int. J. Electrochem. Sci., 16 **(2021)** Article ID: 210334, doi: 10.20964/2021.03.24

International Journal of ELECTROCHEMICAL SCIENCE
www.electrochemsci.org

Effect of Additives on Electrodeposition of Zinc from Alkaline Zincate Solution and Their Synergy Mechanism

Zhongwei Zhan[1], *Qi Zhang*[1], *Shuaixing Wang*[2,*], *Xin Liu*[2], *Zhihua Sun*[1], *Kai Zhang*[1], *Nan DU*[2], *Weifa Shu* [2, 3]

[1] Aviation Key Laboratory of Science and Technology on advanced Corrosion and Protection for Aviation Material, Beijing Institute of Aeronautical Materials, Beijing 100095, P. R. China;
[2] School of Materials Science and Engineering, Nanchang Hangkong University, Nanchang 330063, P. R. China
[3] 8511 Research Institute of China Aerospace Science & Industry Group, Nanjing 210017, P. R. China.
[*]E-mail: wsxxpg@126.com

Received: 18 October 2020 / *Accepted:* 30 December 2020 / *Published:* 31 January 2021

The optimization and combination of additives are particularly important for the electrodepsotion of zinc in alkaline zincate solution. In this paper, the effect of NCZA (polyquaternium-2) and NCZB (sodium propargyl sulfonate) and the combination on the electrodeposition behavior of zinc and their synergy mechanism were systematically analyzed by potentiodynamic polarization, cyclic voltammetry, chronoamperometry, SEM and FT-IR. The results showed that the two additives had different effects on the electrodeposition of zinc. In the basic solution, the electrocrystallization of zinc followed the three-dimensional instantaneous nucleation. NCZB did not change the nucleation mechanism of zinc, and mainly played a leveling role. However, NCZA had a great inhibition effect on the electrodeposition of zinc and transformed the growth mechanism of zinc into three-dimensional continuous nucleation. When the two additives were combined, the adsorption effect on the electrode surface was stronger than that added alone, but no new substances were produced in the plating solution. The synergistic effect of the two additives enhanced the function of the characteristic groups on the electrode surface,which made the electrodeposition potential of Zn move significantly negatively, and the crystals of coating were more detailed and bright.

Keywords: alkaline zincate solution; additive; polyquaternium-2; electrodeposition; nucleation mechanism

1. INTRODUCTION

Zinc coating is one of the most economical and effective method to protect steel from corrosion [1, 2]. For a long time, the electrodeposition of zinc in cyanide solutions has been dominant. However, the use of CN^- has been restricted due to its serious harm to human body and environment. In recent, many cyanide-free electrodeposition systems, including potassium chloride bath [2, 3], alkaline zincate bath [4, 5], ammonium salt bath [6] and acidic sulphate bath [7-10] have been gradually proposed and applied. Among them, the performance of alkaline zincate system is closer to that of cyanide bath. However, the alkaline zincate solution does not contain NaCN, so it is necessary to add additives to improve the coating properties [5, 11, 12].

At present, there are many reports on the additives for zinc electrodeposition in non-cyanide bath. Vanillin, polyethylene glycol (PEG), benzylidene acetone, cetyltrimethylammonium bromide (CTAB), gelatin, glycine and amine compounds are the frequently used additives [5, 11-16]. These additives often play different roles in the electrodeposition process due to their different functional groups and structures. Some studies have shown that the alone use of vanillin, PEG or trisodium nitrilotriacetic can increase the overpotential and nucleation rate of zinc and act as leveling agent and brightener [4, 12, 14]; amine compounds are often used to brighten the coating and refine the crystal grain. Besides, in order to obtain the zinc coating with excellent performance, most scholars and manufacturers often add two or more additives into the electrolytes at the same time. Nayaka et al. [8, 9] found that the three substances produced a synergistic effect when CTAB, salicylaldehyde and acetic acid were added simultaneously, and a uniform, smooth and bright zinc coating with a higher preferred orientation were obtained. Fukumoto et al. [12] found that the overpotentials of the charge transfer of Zn deposition and ZnO_2^{2-} ion diffusion increased with the addition of PQ (a quaternary ammonium cation) and QA (a quaternary ammonium salt with a benzene ring). Yuan et al. [5] also found that additive A and additive B had different adsorption effects on the electrode surface, and the addition of additive A and additive B at the same time displayed the strongest inhibition effect and greatly improved the coating quality.

However, in general, the type, composition and ratio of additives for zinc plating are kept confidential no matter what the literature reports or sold by manufacturers, which is not conducive to the application of the non-cyanide plating technique. Besides, most studies only focus on the effect of additives on the electroplating process and coating structure, and there is still no a unified understanding about the synergistic mechanism of combined additives.

As some documents and our previous research had found that polyquaternium-2 can provide sufficient "cathodic polarization" [5, 13], so it was used to the brightener additive (NCZA) in this paper. Besides, sodium propargyl sulfonate (NCZB) was used as leveling agent. In this paper, the effects of two single additives and their content and ratio on the electrodeposition process and nucleation mechanism of zinc were studied systematically by cathodic polarization, cyclic voltammetry and chronoamperometry. In addition, the synergistic action mechanism of the combined additives were analyzed by differential capacitance curve and fourier transform infrared spectroscopy (FT-IR). The research results can provide technical support for the development of plating additives and the application of alkaline zincate plating.

2. EXPERIMENTAL

2.1 Electroplating process

Fe sheets with sizes of 5 ×2.5 cm were used as the samples. The galvanizing process was as follows: rust removal → water washing → alkaline degreasing → water washing → weak acid activation → water washing → alkaline zincate plating → water washing → drying.

Among them, the degreasing solution was prepared by 60-80 g/L NaOH, 35-55 g/L Na_3PO_4, 30-50 g/L Na_2CO_3, 10-20 g/L Na_2SiO_3 and deionized water; and the degreasing temperature and time is 60-70 °C and 1-3 min, respectively. The activation process was to immerse the sample in 10 vol.% sulfuric acid solution for 30 - 60s. The basic solution (S_0) of alkaline zincate plating was composed of 17 g/L ZnO and 150 g/L NaOH. Besides, 12-24 mL/L additive NCZA (polyquaternium-2) and 0.4 - 2.0 mL/ L NCZB (sodium propargyl sulfonate) were added to the basic solution as needed. The electrodeposition experiments were carried out at 30 °C under the current density of 2.5 A/dm^2.

2.2 Electrochemical testing

Potentiodynamic polarization, cyclic voltammetry (CV) and chronoamperometery (CA) were carried out in alkaline zincate solution by CHI604D electrochemical workstation. The tests were performed by using a three-electrode electrochemical cell. A glassy carbon electrode (GCE) with diameter of 3 mm was used as working electrode, a platinum sheet and a saturated calomel electrode (SCE) and were used as the auxiliary electrode and reference electrode, respectively. Prior to testing, the GCE must be polished to the mirror surface by 1 μm, 0.3 μm and 0.05 μm Al_2O_3 powder, and then ultrasonic cleaned and rinsed with distilled water for three times.

Potentiodynamic polarization experiments were performed in a scan rate of 1 mV/s at room temperature. During CV test, the scan rate was 5 mV/s, which first scanned from the open circuit potential (OCP) to -1.90V in the negative direction and then scanned in the reverse direction to OCP. During chronoamperometry test, the starting potential was set as the OCP, the potential was pulsed to the research potential value -1.85 ~ -1.92 V, and the corresponding current-time transient curves (CCTs) were recorded.

2.3 Characterization of the electrolyte and zinc coating

The characteristic functional groups of alkaline zincate solution without and with different additives were analyzed by Fourier transform infrared spectroscopy (FTIR) using a Bruker Vector 70 FTIR spectrometer.

The microstructure of zinc coating was observed by scanning electron microscope (SEM, QUANTA-200). The surface roughness (R_a) of zinc coating was measured using a surface profile meter (SJ-310). Besides, the adhesion between zinc coating and the substrate was measured by the acoustic signal method using a single scratch tester (WS-2005). The load at which the coating was removed from the substrate was designated as the critical load (L_C) and the moment was recorded by an acoustic emission (AE) signal.

3. RESULTS AND DISCUSSION

3.1 Effect of combined additives on cathodic polarization behavior

Fig. 1(a) shows the cathodic polarization curves of GCE in alkaline zincate solution with different concentrations of NCZA. It can be seen that the precipitation of Zn in the basic solution was easier, the precipitation potential (the point of rapid current growth in the figure) was about -1.54 V. The deposited coating was rough, loose and dull. When NCZA was added into the electrolyte, the polarization curve obviously shifted negatively, and the deposition potential of zinc decreased, indicating that NCZA could be adsorbed on the cathode surface to form a compact adsorption layer and prevented the discharge process or surface diffusion of the zinc complex ion. In addition, the increasing range of cathodic polarization had a positive correlation with NCZA concentration. In order to ensure the uniformity and fineness of zinc coating, the content of NCZA could be controlled at 16 -20 mL/L.

Fig. 1(b) is the cathodic polarization curve of GCE in alkaline zincate solution with different concentrations of NCZB. It could be found that the effect of NCZB on the cathodic polarization was not obvious, only a little negative shift appeared on the polarization curve when NCZB was added alone.

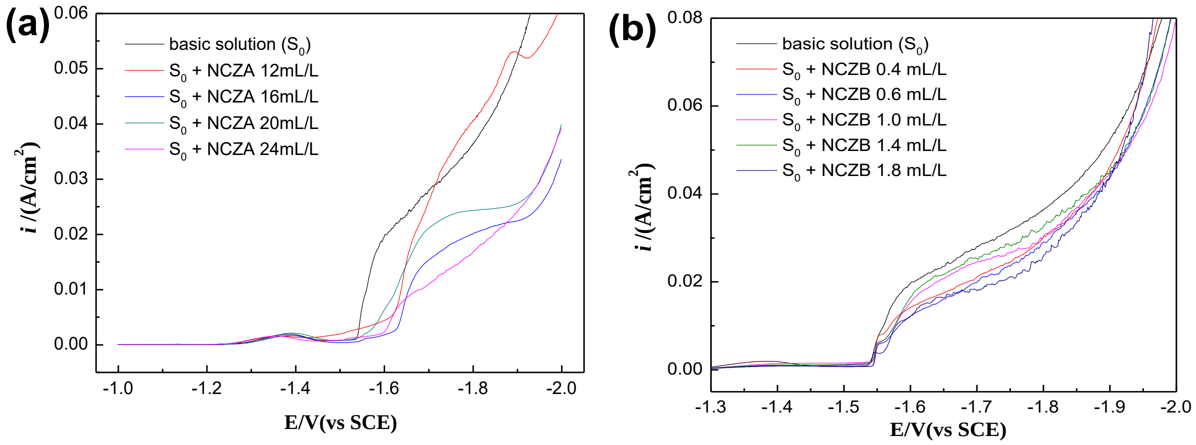

Figure 1. Cathodic polarization curves of GCE in alkaline zincate solution with different concentrations of additives: a) NCZA and b) NCZB

Fig. 2 shows the cathodic polarization curve of GCE in alkaline zincate solution containing both NCZA and NCZB. Comparing with Fig. 1, it could be seen that when NCZA and NCZB were combined into the basic solution, the negative displacement of the cathodic polarization curve was greater. In addition, the cathodic polarization degree of the solution increased as the content of combined additives increased.

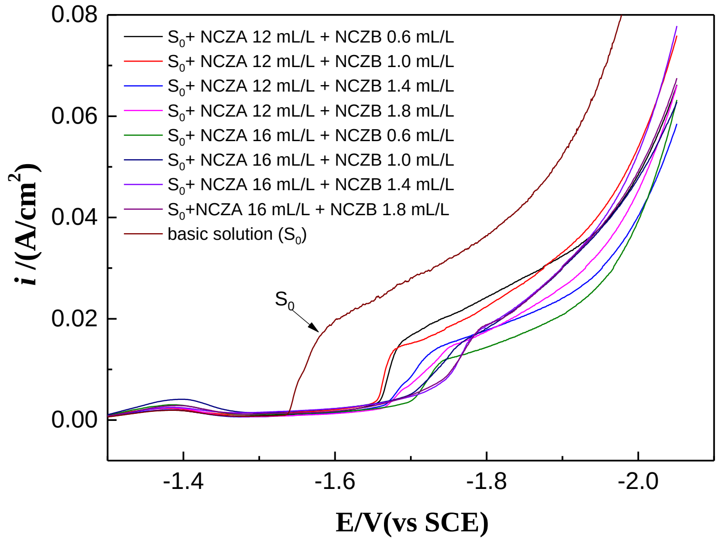

Figure 2. Cathodic polarization curves GCE in alkaline zincate solution containing NCZA and NCZB

3.2 Effect of combined additives on cyclic voltammetric behavior

Fig. 3 shows the cyclic voltammograms of Zn deposition on GCE from alkaline zincate solution with different additives. As shown in Fig. 3(a), in the basic solution, the discharge current increased rapidly when the potential negatively moved to -1.59 V, indicating that zinc began to deposit and then reached the peak current (I_C) at - 1.64 V. When the curve scanned to -1.92 V, it swept back in the positive direction and would cross the previous curve, which was a typical feature of the nucleation process. Subsequently, the current dropped to 0 at -1.53 V, which defined the crossover potential (E_{co}). The difference between the crossover potential and the nucleation potential was defined as the nucleation overpotential (NOP) [5, 13, 17].

When 1.0 mL/L NCZB was added, NOP value only increased by 1mV comparing with that of the basic solution, indicating that NCZB had almost no inhibition effect on zinc electrodeposition. However, the deposition potential of Zn was significantly negative shifted and NOP obviously increased when NCZA was added into the basic solution. Compared with the basic solution, the NOP increased by about 32 mV after adding 16 mL/L NCZA, indicating that NCZA had a significant inhibition effect on zinc electrodeposition, and this inhibition effect was enhanced with the increase of NCZA content.The inhibition effect was the greatest when NCZA and NCZB were combined into the basic solution. The NOP value was as high as 333 mV in the solution with 16 mL/L NCZA and 1 mL /L NCZB, which was greater than the sum of NOP value when the 16 mL/L NCZA and 1 mL /L NCZB were added alone. That was to say, NCZA and NCZB had a strong synergistic effect.

Some results had confirmed that the inhibition effect was often caused by the adsorption of additives on the cathode surface [5, 13-16, 18-22]. When NCZA was added into the plating solution, it would be adsorbed on the active point of the electrode surface to form an adsorption layer, which hindered the progress of the electrodeposition reaction and increased the overpotential, as demonstrated by the increase of NOP value. As the content of NCZA increased, its inhibition effect on the cathode activation point would also enhance, so the NOP value increased accordingly. When only NCZB was added to the basic solution, the additive adsorption layer could not be effectively formed on the cathode surface, so it had no obvious inhibition effect. If NCZA and NCZB were added in combination, a denser adsorption layer would be formed on the cathode surface due to the synergistic effect of the two, its inhibition effect on zinc electrodeposition was greater than that when NCZA or NCZB were added alone. In other words, the combination of the two additives would produce a synergistic effect, rather than a simple addition of them.

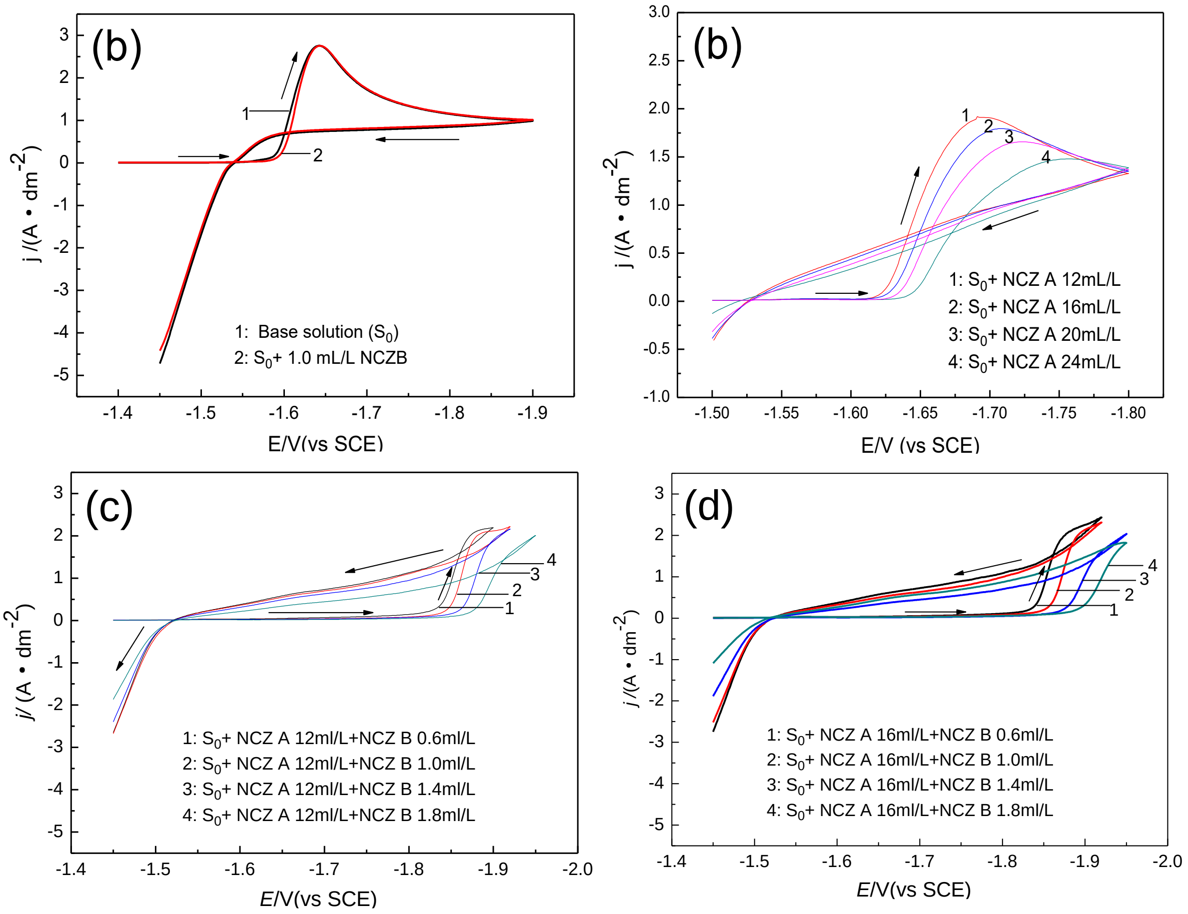

Figure 3. Cyclic voltammograms of Zn deposition on GCE from alkaline zincate solution with different additives: (a) without additive and 1.0 mL/L NCZB; (b) 12~24 mL/ L NCZA ; (c)12mL/L NCZ A + 0.6~1.8mL/L NCZ B; (d) 16mL/L NCZA +0.6~1.8mL/L NCZB

3.3 Effect of combined additives on electrochemical nucleation of zinc

The obvious "inductive current loop" appeared in the cyclic voltammograms, which indicated that the electrodeposition of zinc in alkaline zincate system had undergone the process of crystal nucleation [8, 13, 23, 24]. In this paper, chronoamperometry was used to study the effect of different additives on the electrocrystallization mechanism of zinc.

Fig. 4 shows the current transient curves on the GCE from alkaline zincate system with different additives at - 1.90 V. According to the dimensionless equations of instantaneous nucleation and continuous nucleation in the three-dimensional nucleation process of electrocrystallization proposed by Scharifker [25], the graph of dimensionless $I^2/I_m^2 \sim t/t_m$ could be drawn theoretically.

$$\frac{I^2}{I_m^2} = \frac{1.9542}{t/t_m}[1-\exp(-1.2564\frac{t}{t_m})]^2 \ldots\ldots\ldots(Ins\tan\tan eous) \qquad (1)$$

$$\frac{I^2}{I_m^2} = \frac{1.2254}{t/t_m}[1-\exp(-2.3367\frac{t}{t_m})]^2 \ldots\ldots\ldots\ldots(\mathrm{Pr}\,ogressive) \qquad (2)$$

If the data in Fig. 4 (a) (b) (c) (d) were treated with the same dimensionless processing, and the corresponding graph of $I^2/I_m^2 \sim t/t_m$ could be drawn and shown in Fig. 5 (a) (b) (c) (d).

As shown in Fig. 5(a), the dimensionless curve of $I^2/I_m^2 \sim t/t_m$ for zinc electrocrystallization in the basic solution was relatively close to the instantaneous nucleation theoretical curve, indicating that the electrocrystallization of zinc followed the instantaneous nucleation mechanism [23-26]. When NCZB was added to the basic solution, the dimensionless curve of $I^2/I_m^2 \sim t/t_m$ was still close to the instantaneous nucleation theoretical curve (Fig.5a), indicating that NCZB did not change the nucleation mechanism of zinc. However, the dimensionless curve of $I^2/I_m^2 \sim t/t_m$ was obviously closer to the progressive nucleation theoretical curve when NCZA was added into the basic solution, as shown in Fig. 5(b), which indicated that the nucleation of zinc deposition in the presence of NCZA obeyed a progressive growth mechanism. That was to say, NCZA changed the nucleation mechanism of zinc. Besides, the growth mechanism also followed the progressive nucleation model when the two additives were together added to the basic solution, as shown in Fig. 5(c) and (d).

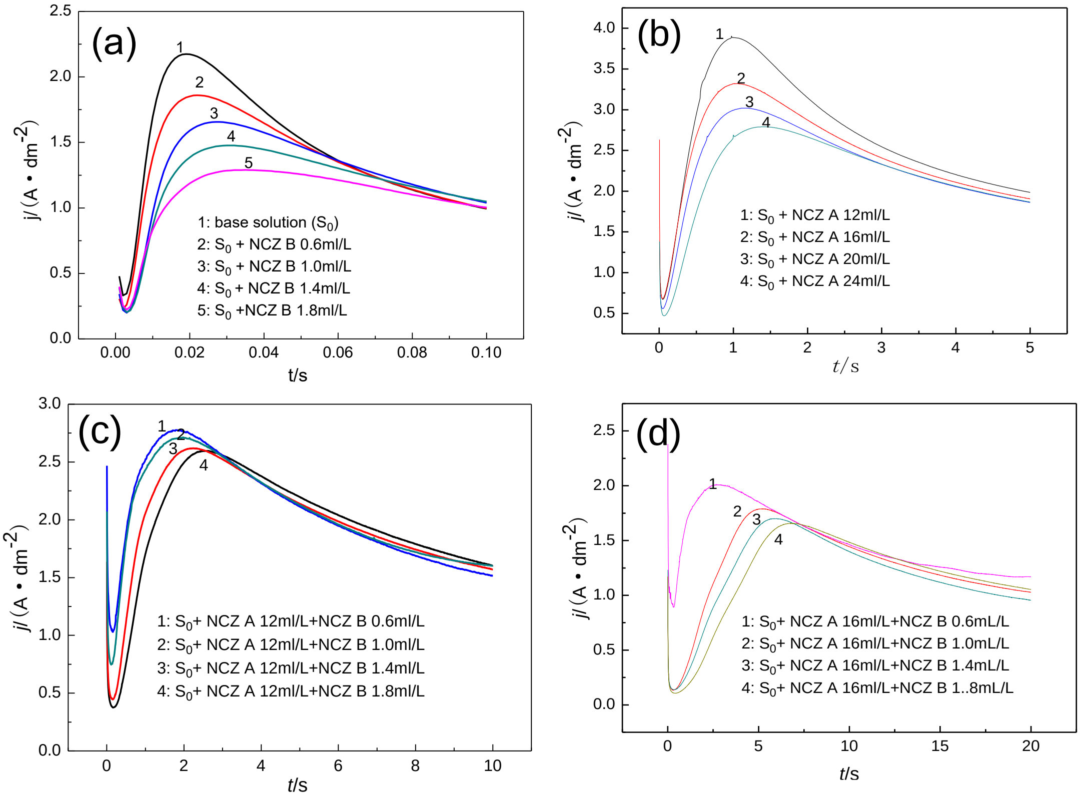

Figure 4. Current transient curves on the GCE from alkaline zincate solution with different additives: (a) without additive and 0.6~1.8 mL/L NCZB; (b) 12~24 mL/ L NCZA ; (c)12mL/L NCZ A + 0.6~1.8mL/L NCZ B; (d) 16mL/L NCZA +0.6~1.8mL/L NCZB

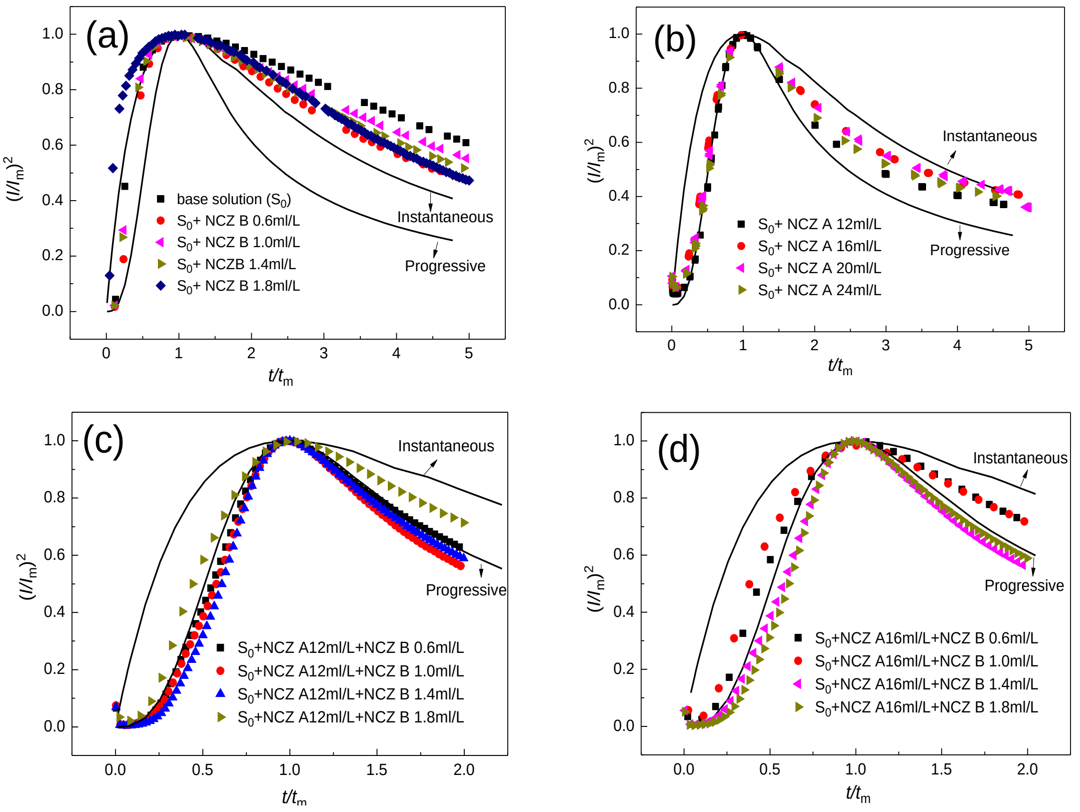

Figure 5. The non-dimensional plots of $I^2/I_m^2 \sim t/t_m$ for electrodeposition of zinc from the alkaline zincate system with different additives: (a) without additive and 0.6~1.8 mL/L NCZB; (b) 12~24 mL/ L NCZA ; (c)12mL/L NCZ A + 0.6~1.8mL/L NCZ B; (d) 16mL/L NCZA +0.6~1.8mL/L NCZB

Table 1 gives the kinetic parameter of the current transient curves for Zn electrodeposituion under different electrolytes and deposition potentials. It can be seen that the $I^2_m t_m$ at each potential in the basic solution hardly changed with the change of step potential, indicating that the crystallization of zinc had undergone three-dimensional growth [25-27]. $I^2_m t_m$ also did not change with the change of step potential when the content of NCZA was constant, showing that the crystallization of zinc also experienced three-dimensional growth in the presence of NCZA. Besides, $I^2_m t_m$ also had the same rule in the electrolytes with NCZB and two additives.

Based on the above analysis, it could be determined that the nucleation of Zn in the basic solution followed a three-dimensional instantaneous model. The additive NCZB did not change the nucleation mechanism of Zn deposition. However, the additive NCZA changed the nucleation mechanism of Zn, which followed a three-dimensional progressive nucleation mechanism. The nucleation mechanism of Zn in the solution containing two additives was the same as when NCZA was added alone, and it also proceeded the three-dimensional progressive growth model.

Table 1. Kinetic parameter analysis of current transient curves for Zn electrodeposition under different electrolytes and deposition potentials.

electrolyte	E (V)	t_m (s)	$10^2 I_m$ (A • cm^{-2})	$10^4 I_m^2 t_m$ (A^2 • s • cm^{-2})	$10^6 D$ (cm • s^{-1})	$10^5 N_0$ (cm^{-2})
Basic solution (S_0)	-1.85	0.024	26.08	16.32	6.41	124.07
	-1.88	0.022	27.65	16.81		132.38
	-1.90	0.019	30.08	17.19		147.35
	-1.92	0.016	33.20	17.64		177.18
S_0 + 12 mL/L NCZA	-1.85	1.11	3.57	14.14	3.11	3.11
	-1.88	0.99	3.61	12.90		3.82
	-1.90	0.92	3.82	13.43		3.95
	-1.92	0.79	3.97	12.58		4.97
S_0 + 16 mL/L NCZA	-1.85	1.22	3.03	11.20	2.66	3.58
	-1.88	1.07	3.31	11.72		3.90
	-1.90	0.91	3.44	10.77		4.48
	-1.92	0.93	3.55	11.72		4.99
S_0 +20 mL/L NCZA	-1.85	1.32	2.80	10.34	2.46	3.58
	-1.88	1.14	3.03	10.47		4.10
	-1.90	1.09	3.15	10.82		4.15
	-1.92	1.00	3.22	10.82		4.72
S_0 + 24 mL/L NCZA	-1.85	1.50	2.50	9.38	2.32	3.23
	-1.88	1.40	2.78	10.82		3.44
	-1.90	1.21	2.90	10.17		3.97
	-1.92	0.89	3.23	9.29		5.92
S_0 + 0.6 mL/L NCZB	-1.85	0.028	21.96	14.45	5.60	127.76
	-1.88	0.027	23.28	14.96		118.16
	-1.90	0.022	26.32	15.47		141.42
	-1.92	0.017	28.80	14.46		193.52
S_0 + 1.0 mL/L NCZB	-1.85	0.033	20.53	13.97	5.40	105.54
	-1.88	0.029	22.15	14.36		116.17
	-1.90	0.027	23.43	15.16		116.68
	-1.92	0.021	25.76	13.80		170.09
S_0 +1.4 mL/L NCZB	-1.85	0.039	18.04	12.87	5.03	96.00
	-1.88	0.033	20.45	14.17		101.64
	-1.90	0.030	20.90	13.33		120.11
	-1.92	0.027	21.69	12.89		138.26
S_0 +1.8 mL/L NCZB	-1.85	0.043	16.31	11.68	4.43	95.27
	-1.88	0.038	17.62	12.05		104.29
	-1.90	0.033	18.25	11.27		128.13
	-1.92	0.032	19.30	12.01		126.04
S_0 + 12 mL/L NCZA + 0.6 mL/L NCZB	-1.85	3.16	2.39	18.08	3.45	0.85
	-1.88	3.03	2.40	17.54		0.92
	-1.90	2.85	2.43	16.89		1.01
	-1.92	2.77	2.50	17.44		1.01
S_0 + 12 mL/L NCZA + 1.0 mL/L NCZB	-1.85	4.65	2.27	24.05	3.24	0.44
	-1.88	4.13	2.30	21.84		0.54
	-1.90	3.92	2.28	20.54		0.61

	-1.92	3.68	2.41	21.48		0.62
S_0 + 12 mL/L NCZA + 1.4 mL/L NCZB	-1.85	5.8	2.22	28.75	3.23	0.29
	-1.88	5.02	2.22	24.75		0.39
	-1.90	4.58	2.24	23.08		0.46
	-1.92	4.36	2.37	24.50		0.56
S_0 + 12 mL/L NCZA + 1.8 mL/L NCZB	-1.85	6.54	2.03	27.16	3.08	0.27
	-1.88	5.52	2.13	25.21		0.35
	-1.90	5.17	2.18	24.62		0.38
	-1.92	5.2	2.28	27.20		0.40
S_0 + 16 mL/L NCZA + 0.6 mL/L NCZB	-1.85	3.03	1.96	11.69	3.45	1.37
	-1.88	2.86	2.02	11.76		1.45
	-1.90	2.63	2.17	12.44		1.49
	-1.92	2.92	2.23	12.09		1.50
S_0 + 16 mL/L NCZA + 1.0 mL/L NCZB	-1.85	6.12	1.71	17.98	3.24	0.44
	-1.88	5.65	1.73	17.09		0.51
	-1.90	5.27	1.79	16.89		0.55
	-1.92	5.16	1.82	16.67		0.57
S_0 + 16 mL/L NCZA + 1.4 mL/L NCZB	-1.85	7.21	1.58	17.99	3.23	0.32
	-1.88	6.60	1.63	17.53		0.38
	-1.90	6.05	1.69	17.27		0.48
	-1.92	5.69	1.73	17.03		0.69
S_0 + 16 mL/L NCZA + 1.8 mL/L NCZB	-1.85	7.82	1.61	20.27	3.08	0.31
	-1.88	6.99	1.67	19.49		0.33
	-1.90	6.81	1.70	19.68		0.37
	-1.92	6.34	1.74	19.19		0.41

It can also be seen from Table 1 that the peak current (I_m) of the current transient curve at the same potential decreased sequentially, and the time taken to reach the peak current (t_m) increased in accordance with the order of the basic solution (S_0), S_0+ NCZB, S_0+ NCZA and S_0+ NCZA +NCZB; indicating that the nucleation process of Zn was inhibited by the additives in different degrees.

According to the Scharifker-Hills model [25], the nucleation density (N_0) at the initial stage of electrodeposition could be calculated by Eq. (3).

$$N_0 = 0.0652 \frac{1}{(8\pi C_0 V_m)^{\frac{1}{2}}} \left(\frac{nFC_0}{I_m t_m}\right)^2 \qquad (3)$$

Where, V_m is the molar volume, I_m is the peak current and t_m is the nucleation relaxation time.

The nucleation density under different conditions calculated by Eq. 3 was also shown in Table 1. As shown in Table 1, the nucleation density in the absence of NCZA was much higher than that with NCZA, meanwhile, the nucleation density would increase with the increase of NCZA content.

As the above analysis, the nucleation of Zn in the basic solution followed the three-dimensional instantaneous model, that was, all the active points were transformed into crystal nuclei at the beginning of zinc deposition [25]. However, the electrocrystallization of Zn followed a three-dimensional progressive mechanism after adding NCZA, that was, the nucleation density increased with the extension of deposition time [23-27]. Therefore, the nucleation density in the basic solution was very large, but the nucleation density was lower after adding NCZA. When NCZB was added to the basic solution, the nucleation density decreased with the increase of NCZB content, and the two were in inverse proportion. The nucleation density at the same potential was the smallest when NCZA and NCZB were added simultaneously. Interestingly, NCZA and NCZB still maintained their respective effects on the nucleation density when the two additives are used together; NCZA increased the nucleation density, while NCZB was the opposite. A reasonable explanation was that NCZA was adsorbed on the electrode surface and increased the overpotential of zinc electrodeposition, so the nucleation density in the initial stage of deposition increased with the increase of NCZA content. NCZB mainly acted as a leveling agent during the electroplating process, which might be adsorbed on the low potential points on the electrode surface and covered the active sites, resulting in a decrease in nucleation density.

3.4 Adsorption behavior of combined additives on electrode surface

In order to verify the previous hypothesis on the synergistic effect of the two additives, the adsorption behavior of the two additives on the electrode was studied by the differential capacitance test, and the results were shown in Fig. 6.

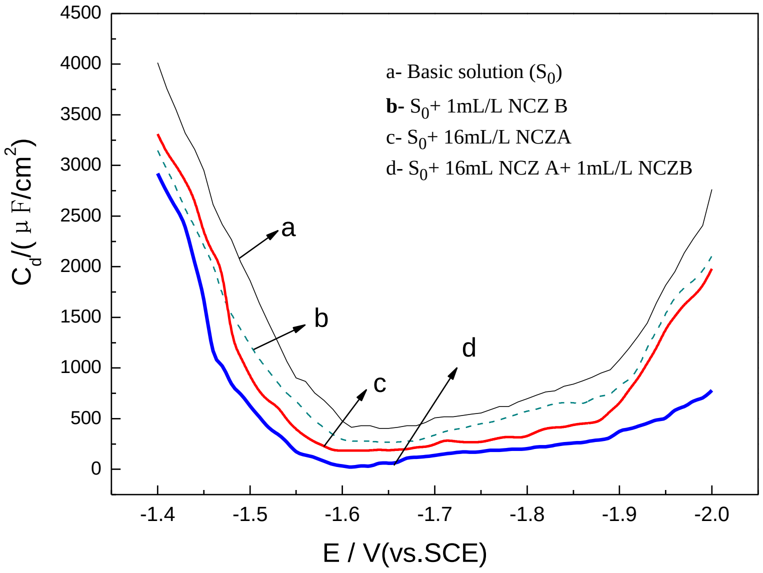

Figure 6. Differential capacitance curves of four solutions adsorbed on the surface of zinc coating

As shown in Fig. 6, the differential capacitance of basic solution was greater than that of the electrolyte containing additives, showing that the water molecules at the electrode-solution interface were pushed out by organic molecules. In general, the volume of organic molecules was relatively larger, the differential capacitance would decrease as the thickness of the electrical double layer (d) increased according to the Eq. (4).

$$C_d=\varepsilon_0\cdot\varepsilon_r/d \qquad (4)$$

where ε_0 represents the vacuum permittivity and ε_r represents the relative permittivity. In addition, the relative dielectric constant of organic molecules was smaller than that of water molecules, so the differential capacitance of the electrode would be reduced if they adsorbed on the electrode surface.

The differential capacitance values of zinc-coated electrodes measured at different potentials in the four electrolytes are shown in Table 2. According to Fig. 6 and Table 2, the differential capacitance of the electrode decreased to a certain extent when NCZB or (and) NCZA were added to the basic solution. Besides, the differential capacitance value of the system containing NCZA is about 100 ~ 200 μF/cm^2 smaller than that of the solution with NCZB at the same potential, indicating that NCZA had a stronger adsorption effect on the electrode surface. However, the differential capacitance value at each potential in the solution with two additives was significantly lower, and the decrease degree was greater than the two was added alone. It showed that the adsorption effect on the electrode surface when the two additives existed in the solution was not the simple co-adsorption of two additive molecules, but the synergistic effect between the two additives, thereby increasing the adsorption capacity or the coverage on the electrode surface.

Some researches had confirmed that the adsorption of additive molecules was simply the adsorption of the heterogeneous groups on the electrode surface if there was only one additive in the solution, and only part of the active points could be covered [11-14, 21, 22]. However, the two additives not only performed the simple group adsorption on the electrode surface, but also they had the mutual influence when the two simultaneously acted [5, 8-10]. One of the additive molecules occupied some adsorption active points, and the other additive occupied the remaining active points by changing the way of spatial adsorption, which made the adsorption layer denser and greatly reduced the active points for the reduction of zinc ions. Therefore, the presence of the two additives in the electrolyte could significantly increase the polarization effect and the nucleation overpotential, and finally obtained a fine, bright and flat coating.

Table 2. Differential capacitance values of zinc-coated electrode in the four electrolytess

Potential	C_d (μF/cm^2)			
	basic solution (S_0)	S_0 + 1mL/L NCZB	S_0+ 16mL/L NCZA	S_0+ 16mL/L NCZ +1mL/L NCZB
-1.4	4014.38	3146.83	3310.0	2920.0
-1.5	1861.03	1226.56	914.94	625.77
-1.6	474.17	288.88	185.01	33.41
-1.7	507.86	336.60	243.96	137.04
-1.8	696.79	578.04	322.57	202.25
-1.9	1080.85	833.52	643.46	372.82

3.5 Infrared spectra of the electrolyte with combined additives

In order to further explore the principle of synergistic effect of NCZA and NCZB, the infrared spectra of five electrolytes (the above four electrolytes and the electrolyte containing two additives that had been energized 20A·h) were tested using FTIR and the test results were shown in Fig. 7. As shown in Fig. 7(a), no new peaks appeared on the basis of the original NCZA and NCZB, when the two additives were added simultaneously. All the characteristic absorption peaks for the electrolytes containing two additives were present in the electrolytes with NCZA or NCZB alone, which indicated that the simultaneous addition of two additives did not form new groups through the interaction between chemical bonds, but increased the peak intensity of the original groups.

For example, at the wavelength of 864.09 cm^{-1} (the vibration absorption peak of N-O bond [28]), the infrared transmittance of the solution with two additives was much lower than that when the two additives were added alone, showing that the together addition of two additives made this group strengthen the absorption for light in this wavelength on the original basis.

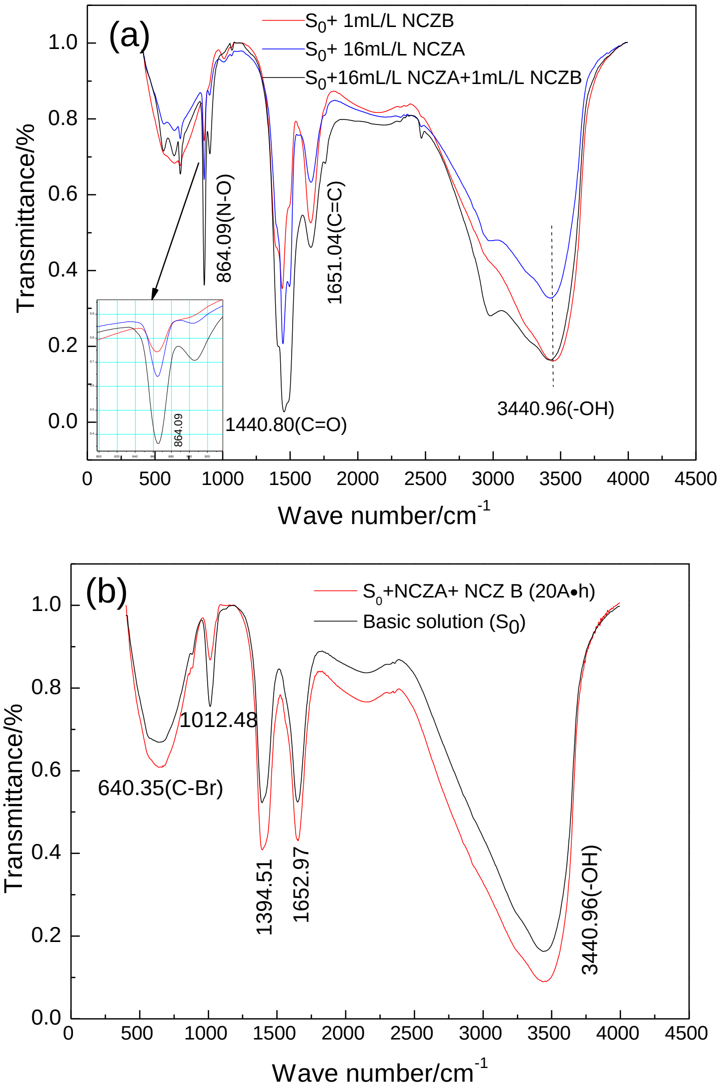

Figure 7. FTIR spectra of different electrolytes: (a) S_0 with NCZA, S_0 with NCZB, S_0 with two additives; (b)S_0, S_0 with two additives after using for 20A·h

The reason may be that the atoms in the molecule produced a steric hindrance effect through a synergistic effect when the two additives were present simultaneously, which reduced the reactivity of the group and changed the dipole moment, thereby enhancing the absorption for light. In addition, the same strengthening effects were observed at the wave number of 1440.80 cm^{-1} (the stretching mode of

C = O bond in carboxyl group [28]) and 1651.04 cm^{-1} (ester group containing C = C double bond [28]). This strengthening effect made NCZA and NCZB have a synergistic effect to better adsorb on the electrode surface when two additives were added simultaneously, so that a bright and uniform coating was obtained.

Besides, it can be seen from Fig. 7(b) that the infrared spectrum of the solution with two additives after using for 20A·h was very similar to that of the basic solution (S_0). There was almost no difference except for the slight difference in the peak intensity at the absorption peak, and the characteristic absorption peaks of NCZA and NCZB could no longer be observed, indicating that these two additives were almost completely consumed during the electrodeposition process.

3.6 The microstructure and adhesion of zinc coating

Fig. 8 shows the surface morphology of zinc coatings obtained in different electrolytes. Table 3 gives the surface roughness (Ra) and the adhesion of different coatings. It can be seen that the effects of two additives on the microstructure of zinc coating were quite different.

As shown in Fig. 8(a), the coating formed in the basic solution was relatively rough, and the outward growth of grains was obvious. Ra value of this coating was up to 6.24 μm, meanwhile, the adhesion between coating and substrate was poor, the critical load (L_C) was only 20.15 N. After adding NCZB, the size of grains for zinc coating was still coarse (Fig. 8b), but the coating adhesion was enhanced to a certain extent. When NCZA was added, the outward growth of grains was inhibited, the grains were obviously smaller and spherical (Fig. 8c), and Ra value dropped to 0.99 μm. Meanwhile, the adhesion of the coating formed in this system was better. When NCZA and NCZB were added simultaneously, the coating had fine crystals (Fig. 8d), the coating surface was smooth and bright, Ra value was only 0.29 μm.

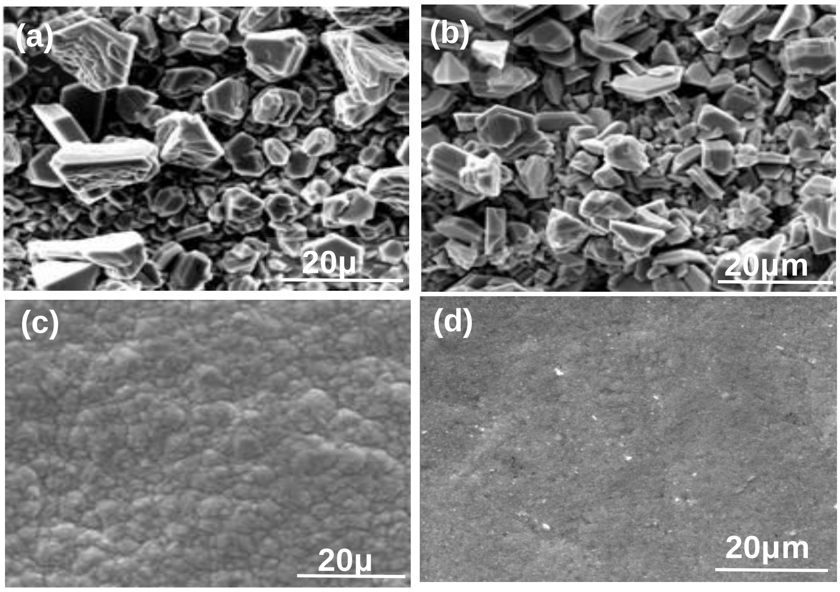

Figure 8. Surface morphology of zinc coatings prepared in different electrolytes (a) basic solution (S_0), (b) S_0+NCZB, (c) S_0+NCZA, (d) S_0+NCZA +NCZB

Based on the above results, it can be determined that NCZA mainly played the role of grain refinement, while NCZB mainly played the role of leveling. No matter which additive was added alone, the coating adhesion was enhanced to a certain extent, and the NCZA was more significant than the NCZB; when the two additives were added at the same time, the coating adhesion mainly depended on the NCZA.

Table 3. Surface roughness and adhesion of zinc coatings formed in eletrolytes with different additives

Electrolyte system	Surface roughness Ra (μm)	Coating adhesion L_C (N)
basic solution(S_0)	6.24	20.15
S_0 +1mL/LNCZ B	6.37	24.05
S_0 +16mL/LNCZ A	0.99	25.65
S_0 +16mL/LNCZ A +1mL/L NCZ B	0.29	25.55

4. CONCLUSION

(1) In the alkaline zincate system, the additive NCZA had an inhibition effect on the cathodic process of zinc electrodeposition, and the inhibition effect would increase as its content increased. However, the additive NCZB mainly played a leveling role. When the two additives worked together, the negative shift of precipitation potential was the most obvious, the size of grains were the smallest, and the coating was bright and fine.

(2) Both NCZA and NCZB could be adsorbed on the electrode surface, but the adsorption effect of NCZA was stronger. When the two additives were combined, the adsorption effect was stronger than that added alone. FTIR results showed that NCZA and NCZB did not produce new substances when they were added together. The two additives generated steric hindrance through the synergistic effect to strengthen the function of the characteristic groups on the electrode surface.

(3) In the basic solution, the nucleation of zinc followed a three-dimensional instantaneous model. The NCZB did not change the instantaneous nucleation mechanism of zinc deposition; while the NCZA could be adsorbed on the electrode surface, and changed the nucleation mechanism of zinc. In the solutions containing NCZA, the growth of zinc followed a three-dimensional progressive nucleation mechanism.

(4) Both NCZA and NCZB could improve the adhesion of zinc coating to a certain extent, but NCZA was more effective. The coating adhesion mainly depended on the additive NCZA when the two additives were added together.

ACKNOWLEDGEMENTS
The authors gratefully acknowledge the financial support of National Natural Science Foundation of China (Grant No. 51401196).

References

1. M. C. Li, L. L. Jiang, W. Q. Zhang, Y. H. Qian, S. Z. Luo, J. N. Shen, *J. Solid State Electrochem.*, 11 (2007) 1319-1325.
2. K. M. S. Youssef, C. C. Koch, P. S. Fedkiw, *Corros. Sci.* 46 (2004) 51-64.
3. E. M. Oliveira, I. A. Carlos, *J. Appl. Electrochem.*, 38 (2008) 1203-1210.
4. M. F. Carvalho, I. A. Carlos, *Electrochim. Acta*, 113 (2013) 229-239.
5. L. Yuan, Z. Y. Ding, S. J. Liu, W. F. Shu, Y. N. He, *Trans. Nonferrous Met. Soc. China*, 27(2017) 1656-1664.
6. Z. M. Xia, S. H. Yang, L. H. Duan, *Int. J. Min. Met. Mater.*, 22 (2015) 682-687.
7. M. C. Li, S. Z. Luo, Y. H. Qian, *J. Electrochem. Soc.*, 154 (2007) D567-D571.
8. K. O. Nayana, T. V. Venkatesha, B. M. Praveen, *J. Appl. Electrochem.*, 41 (2011) 39-49.
9. K. O. Nayana, T. V. Venkatesha, *J. Ind. Eng. Chem.*, 26 (2015) 107-115.
10. K. O. Nayana, T. V. Venkatesha, *J. Electroanal. Chem.*, 663 (2011) 98-107.
11. V. Zuniga, R. Ortega, Y. Meas, *Plat. Surf.Finish.*, 91 (2004) 46-51.
12. K. Fukumoto, S. Oue, Y. Kikuchi, *Mater. Trans.*, 61 (2020) 497-505.
13. N. Soroura, W. Zhang, E. GHali, G. Houlachi, *Hydrometallurgy*, 171 (2017) 320-332.
14. S-J Kim, H-T Kim, S-M. Parka, *J. Electrochem. Soc.*, 151 (2004) C850-C854.
15. M. F. Carvalho, E. P. Barbano, I. A. Carlos, *Electrochim. Acta*, 109 (2013) 798-808.
16. K. D. Song, K. B. Kim, S. H. Han, *Electrochem. Solid St. Lett.*, 7 (2004) 20-24.
17. N. Sorour, W. Zhang, G. Gabra, E. Ghali, G. Houlachi, *Hydrometallurgy*, 157 (2015) 261-269
18. O. Aaboubi, J. Douglade, X. Abenaqui, *Electrochim. Acta*, 56 (2011) 7885-7889.
19. B. Kavitha, P. Santhosh, M. Renukadevi, *Surf. Coat. Technol.*, 201 (2006) 3438-3442.
20. I.L. Lehr, S. B. Saidman, *Appl. Surf. Sci.*, 258 (2012) 4417-4423.
21. W. M. Gu, C. Q. Liu, J. Tang, R Y. Liu, H. Yang, J. H. Hu, *Hydrometallurgy*, 175 (2018) 43-51.
22. M. Pushpavanam, *J. Appl. Electrochem.*, 36 (2006) 315-322.
23. W. J. Peng, Y. Y. Wang, *J. Cent. South Univ. Technol.*, 13 (2006) 637-641.
24. J. Y. Lee, J. W. Kim, M. K. Lee, *J. Electrochem. Soc.*, 2004, 151 (2004) C25-C31.
25. B. Scharifker, S. G. Hill, *Electrochim. Acta*, 28 (1983) 879-889.
26. A.C. Beshore, B.J. Flori, G. Schade, T.J. O'Keefe, *J. Appl. Electrochem.*, 17 (1987) 765-772.
27. N.D. Nikolić, P.M. Živković, J.D. Lović, G. Branković, *J. Electroanal. Chem.*, 785 (2017) 65-74.
28. P. J. Larkin, Infrared and Raman Spectroscopy: Principles and Spectral Interpretation (2nd Edition), *Elsevier*, 2018.